IEEE Photonics Journal
An IEEE Photonics Society Publication

Open Access

Use of Finite Light Sources to Develop Continuous-Phase Visual Optics

Volume 4, Number 6, December 2012

Jyun-Jie Sie
Yu-Ju Liu
Chih-Tsung Chang
En-Hung Lin
Po-Lei Lee
Kuo-Kai Shyu, Member, IEEE

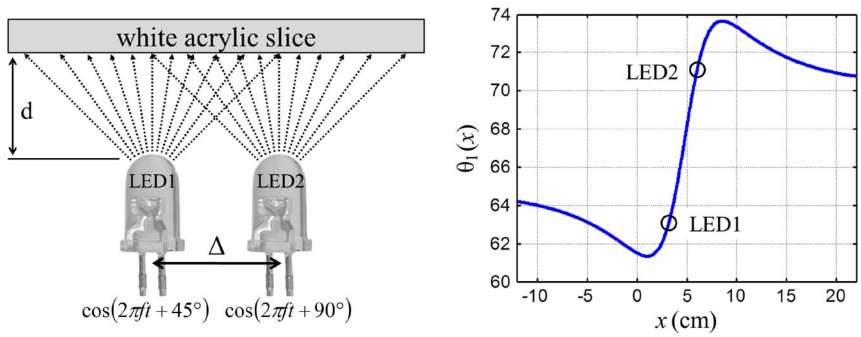

DOI: 10.1109/JPHOT.2012.2232650
1943-0655/$31.00 ©2012 IEEE

Use of Finite Light Sources to Develop Continuous-Phase Visual Optics

Jyun-Jie Sie, Yu-Ju Liu, Chih-Tsung Chang, En-Hung Lin, Po-Lei Lee, and Kuo-Kai Shyu, ***Member, IEEE***

Department of Electrical Engineering, National Central University, Jhongli City 32001, Taiwan

DOI: 10.1109/JPHOT.2012.2232650

Manuscript received October 21, 2012; revised December 3, 2012; accepted December 3, 2012. Date of current version December 19, 2012. Corresponding author: J.-J. Sie (e-mail: hero0800@gmail.com).

Abstract: Visual optics for brain–computer interfaces (BCIs) has undergone several developments. Currently, visual optics only provides multiple single-light sources, which limit its applications. This study uses several single-light sources to achieve continuous-phase visual optics. This is combined with a liquid-crystal display (LCD) panel to develop an interactive instrument. Although light synthesis is a nonlinear process, the nonlinear problem is solved by increasing the number of light sources. The measurement data confirm that the phase is approximately linear. This interactive instrument is useful in the biomedical engineering field because it predicts user gaze location.

Index Terms: Visual optics, brain–computer interface (BCI), continuous phase, biomedical engineering.

1. Introduction

Visual evoked potential (VEP) has been used to diagnose a function of frequency from both normal users and glaucoma patients with asymmetric visual-field loss in various stages of the disease [1]. VEP has the characteristic of being dominated by the response induced from the visual stimulus located at the user's central visual field [2]–[5], which is called "cortical magnification" [4], [5]. In the biomedical engineering field, visual optics used in brain–computer interfaces (BCIs), generally referred to as VEP-based BCIs, has undergone several developments [6], [7]. This system helps patients with diseases such as amyotrophic lateral scleroses, and it allows users to control external devices or express their intentions independent of peripheral neuromuscular functions. BCIs use visual optics to evoke an electroencephalogram (EEG). Different visual-optic characteristics yield different EEG results. Studies [8]–[14] have used frequency-encoding techniques to implement a VEP-based BCI to assist patients in achieving mobility. To achieve the same goal, Sellers *et al.* [15] used a liquid-crystal display (LCD) screen with event-related potential to evoke EEGs. References [16] and [17] also developed visual optics for flash visual-evoked potential. Studies usually use frequency encoding to derive phase encoding [18], [19]. This method has several advantages, including its simple system structure, fast response, and high accuracy. Several studies [18]–[21] have developed an online BCI based on phase encoding.

Visual optics currently only provides multiple single-light sources (option). This means that visual optics conveys a fragmented result. For example, visual optics can be used to control cursor direction (left or right) but cannot control cursor-moving distance. Moving a cursor a certain distance using the traditional method requires more time, but the method proposed in this study instantly locates the cursor. The traditional methods and the proposed method exhibit digital control {0, 1} and analog control [0, 1] differences. This study produces a continuous-phase visual optics system.

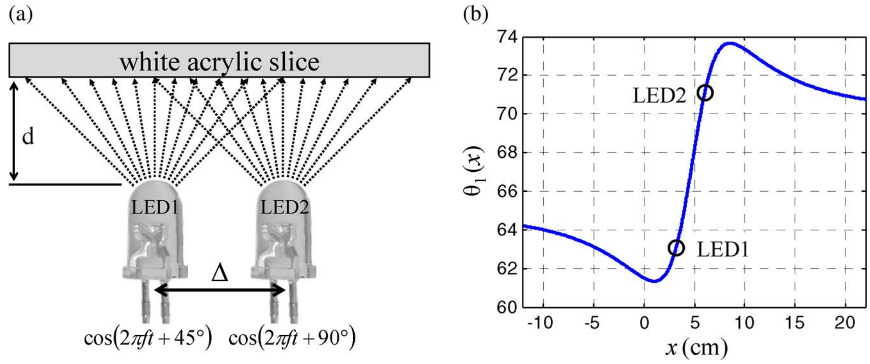

Fig. 1. (a) Synthetic light to produce a continuous-phase visual optics illustration. (b) Simulation result.

The continuous-phase system is used in a backlit module and combined with an LCD panel to form an interactive BCI. This system integrates visual optics with a display interface in the same field of view, facilitating use and menu design. This study examines a visual stimulator and its simulation, implementation, and measurement results.

2. Principle of Visual Optics and Simulation

A previous study [18] proposed phase-encoding visual optics. Phase encoding divided signals into eight phases, and a separate LED displayed each phase. In other words, the system provided eight options to the user. The light sources of the eight LEDs did not interfere with each other in space. This study develops the reverse of this operation, using light sources from adjacent LEDs to synthesize the other phases, as shown in Fig. 1. Fig. 1(a) shows that the light sources of adjacent LEDs overlap, and the lights are projected onto a white acrylic slice. Using different phases and (1) to synthesize other phases, $a(x)$ is the single-light source projection intensity on the white acrylic slice, and x is a position on the white acrylic slice. Simulation result $\theta_1(x)$ is the relationship between phase and position, shown in Fig. 1(b), where $\text{d} = 3.2$ cm, and $\Delta = 3.2$ cm is the interval between LEDs. Thus

$$E_1(t,x) = a(x)e^{-j(2\pi ft+45^\circ)} + a(x-\Delta)e^{-j(2\pi ft+90^\circ)} = a_1(x)e^{-j(2\pi ft+\theta_1(x))} \tag{1}$$

$$\theta_1(x) = \arctan\left[\int E_1(t,x)e^{j2\pi ft}dt\right]. \tag{2}$$

Fig. 1 shows that (1) represents the synthetic light phase, where t is time, $E_1(t,x)$ is the intensity relationship between time and position on the white acrylic slice, and $a_1(x)$ is the synthetic intensity on the white acrylic slice. To simulate the accuracy of the results, $a(x)$ for normalization is obtained by measurements, as shown in Fig. 2(a). $\theta_1(x)$ is obtained using (2). $\theta_1(x)$ is a function of x, and it experiences a phase change because of differences in position x. If the continuous phase is synthesized from two light sources, $\theta_1(x)$ returns a nonlinear result, as shown in Fig. 1(b). Although the phase between LED1 and LED2 seems to be linear, it uses a range that is smaller than expected (i.e., not between 45° and 90°). However, to achieve a linear result and expand the phase range, the number of LEDs must increase. Therefore, the 360° phase angle is divided into eight equal portions, based on suggestions in the literature [18]. The phase angles used are 45°, 90°, 135°, 180°, 225°, 270°, 315°, and 360°. The continuous-phase margin causes nonlinearity problems, for example, at 45° and 360°. To obtain a more linear range, the number of LEDs on two sides of the continuous phase was increased. The final phase results are 0°, 45°, 90°, 135°, 180°, 225°, 270°, 315°, 360°, and 405°. Equation (3) calculates the synthetic intensity from 10 different phase LEDs, where $t = 0$ s and $\Delta = 3.2$ cm. Fig. 2(b) and (c) shows the simulation results. Fig. 2(b) shows the light intensity of $E_2(t,x)$, and o represents the LED locations. Because the light intensity of the backlit module must be consistent, a range of $x = 5$ to 30 cm was used. The system must also consider actual use, which means that the phase is in the linear region. Phase $\theta_2(x)$ is

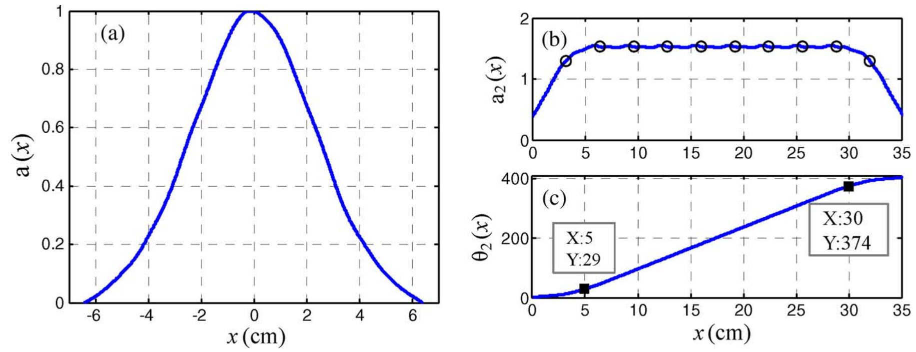

Fig. 2. (a) Measured light intensity distribution curve of a single LED. Using the results in (a), the (b) simulated synthetic light intensity, and the (c) continuous-phase distribution curve; the *o* symbols represent the LED locations.

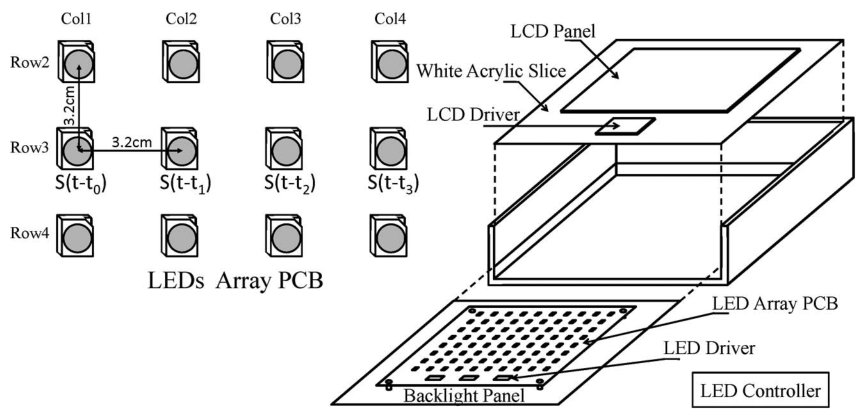

Fig. 3. Device with the visual optics of the LCD screen.

calculated using (2). Fig. 2(c) shows that only $x = 5$ to 30 cm reflects a linear phase. Based on these conditions, the LCD panel should be placed at $x = 5$ to 30 cm, in other words, between the second (45°) and ninth LEDs (360°). The simulation results in Fig. 2(c) reflect a linear phase. Differential calculus is used to understand this linearity. Thus

$$E_2(t,x) = \sum_{i=0}^{9} a(x - i \cdot \Delta) e^{-j(2\pi ft + 360/8 \times i)} = a_2(x) e^{-j(2\pi ft + \theta_2(x))}. \tag{3}$$

3. Implementation

The VEP-based BCI [6], [8]–[10], [17]–[21] contains visual optics and an output device. The output device function represents user choices. This study uses a 15-in LCD screen to create the visual optics and output device. The BCI system output device is an LCD panel, and the visual optics is a backlit module. The backlit module must use phase coding; therefore, backlit modules must be produced. Of the LCD screen, only the LCD panel and the LCD drive were retained; the backlit module and the LED controller were added. The white LED was used as the backlight, and it was a surface-mounted device package type. The LEDs were arranged in an array (10 : 8) according to the size of the LCD screen, as shown in Fig. 3. Most LEDs in the array were used as a backlight. Only the third LED array row was used to realize visual optics that contained phase encoding, as shown in the LED array PCB (Printed Circuit Board) in Fig. 3. Frequency selection was based on suggestions in the literature [22], and its maximal amplitude was almost 22.8 Hz, and it used square waves to drive the LEDs. The square wave is a simple and easy method of implementing phase

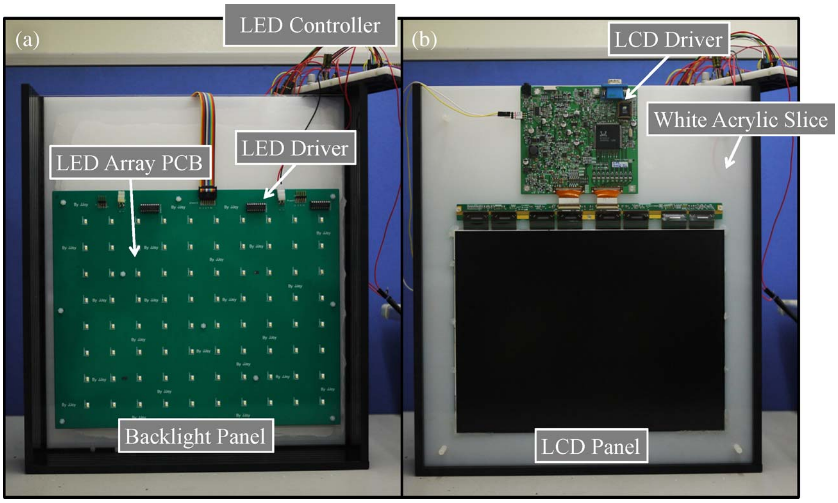

Fig. 4. Hardware with the visual optics of the LCD screen.

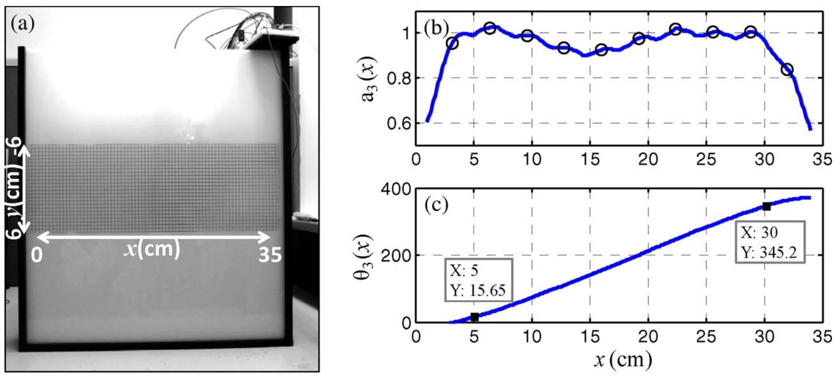

Fig. 5. (a) White acrylic slice of the system is marked with a grid of 0.5 cm $\times$ 0.5 cm squares. At $y = 0$ on the white acrylic slice, the (b) light intensity and (c) phase were measured.

encoding [18], which requires an additional trigger event for the extraction phase. $S(t)$ represents square wave $S(t - t_0)$, $t_0 = 0$ s represents 0° square wave $S(t - t_1)$, $t_1 = 1/(22.8 \cdot 8) = 5.48$ ms represents a 45° square wave, and so on. The synthesis of 10 of these signals, $E_3(t, x)$, is calculated using (4). According to the simulation results, LEDs must be spaced 3.2 cm apart, and the backlight must be uniform. Thus

$$E_3(t, x) = \sum_{i=0}^{9} a(x - i \cdot \Delta) S(t - t_i). \tag{4}$$

Fig. 4 shows the hardware architecture of the visual optics for the LCD screen. Fig. 4(a) shows the LED driver, LED array PCB, and LED controller. Fig. 4(b) shows that the LCD panel and the LCD driver are attached to the white acrylic slice.

4. Results

A grid was printed on the white acrylic slice to obtain accurate data, as shown in Fig. 5(a). Each grid square is 0.5 cm $\times$ 0.5 cm. After measuring light intensity on the white acrylic slice, this intensity was normalized. The third row of LEDs in the LED array PCB was defined as located at $y = 0$ in Fig. 5(a). The data were measured based on suggestions from the literature [18]. Light intensity

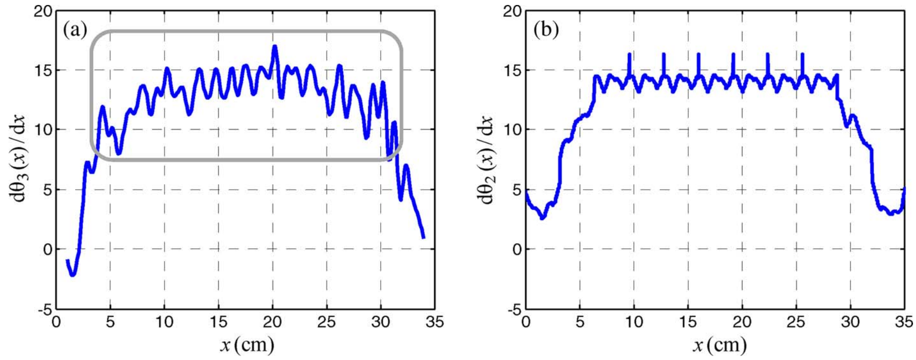

Fig. 6. Using phases $\theta_3(x)$ and $\theta_2(x)$ obtained results of (a) and (b) through differential calculus.

$a_3(x)$ is the sine-wave amplitude, and phase $\theta_3(x)$ is the sine-wave delay time. Fig. 5(b) and (c) shows the results. Fig. 5(b) displays the normalized light intensity, which shows that light intensity is unevenly distributed. Although light intensity distribution deviates slightly, this does not affect the continuous-phase results, as shown in Fig. 5(c). Fig. 5(c) shows the relationship between x and phase $\theta_3(x)$ of the LCD screen. A linear relationship exists between $x = 5-30$ cm. These results are similar to the simulation results. Fig. 5(c) shows that the phase range from 15.65° to 345.2° is the linear range.

In the application of VEP based on BCI, we are more interested in the phase data of LED. The linear phase degree is particularly important. Differential calculus is used to describe the linear degree, and Fig. 6(a) is obtained from Fig. 5(c). Similarly, Fig. 6(b) is obtained from Fig. 2(c). The measurement results and simulation results are similar. The degree of linearity is identified using Fig. 6(a). The two data margins show that the results are not suitably linear; therefore, the BCI system excludes the $x < 5$ and $x > 30$ regions. The simulation results in Fig. 6(b) reflect the same situation. In the $5 < x < 30$ region (gray box), although the measurement result is not a constant, it varies between 10 and 15. Simulation results, such as minor swing, can be tolerated, showing that the results are approximately linear. This shows that the LCD panel was placed at $x = 5$ to 30 cm, which is approximately a linear region.

In VEP-based BCI applications, user gaze is located on an LCD screen. The BCI system obtains EEG phase data $\theta_{EEG}(t)$ by calculating the user's EEG. The EEG phase data are then linearly transformed to estimate user-gazed location x'. However, the estimated result x' and actual result x do not match because the BCI system does not know the LED phase data in Fig. 5(c). Normally, the BCI system requires a user to gaze at two points on the LCD screen to calculate the EEG and x' phase data, where x' is a known location on the LCD screen. The BCI system must obtain two fixed points (phase and x') to calculate the linear equation. For example, using (73.32°, 10) and (283.4°, 25) in Fig. 5(c) allows the calculation of (5). After the BCI system obtains the phase data, it uses mapping to obtain estimated location x'. If the BCI system has the measurement data in Fig. 5(c), it can identify actual location x. If the measurement data are unknown, it must estimate location x'. In order to understand this problem, a known phase was used to obtain the location error using (5) and Fig. 5(c). Subtracting x' from x produces Fig. 7, which shows the error that also approximates the degree. The figure shows that a large error exists at the margin, but this error value is acceptable for user gaze location. The other error values are small. Based on this situation and the use of synthetic light, the method of realizing the linear-phase system is feasible. Thus

$$x' = f(\theta_{EEG}(t)) = 0.0714\theta_{EEG}(t) + 4.765. \quad (5)$$

VEP-based BCI accounts for central visual field offset. In other words, when the central visual field does not focus on $y = 0$, whether the phase results have been affected is unknown. To clarify this situation, the measurement phase results are extended to two dimensions. Fig. 5(a) shows the measurement ranges. Light intensity and phase were measured within the grid, and Fig. 8 shows these results. Fig. 8(a) and (b) shows the same normalized light intensity results, and Fig. 8(c) and (d)

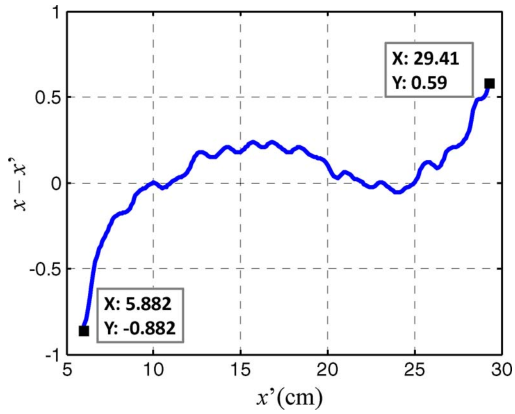

Fig. 7. Error curve of x and x'.

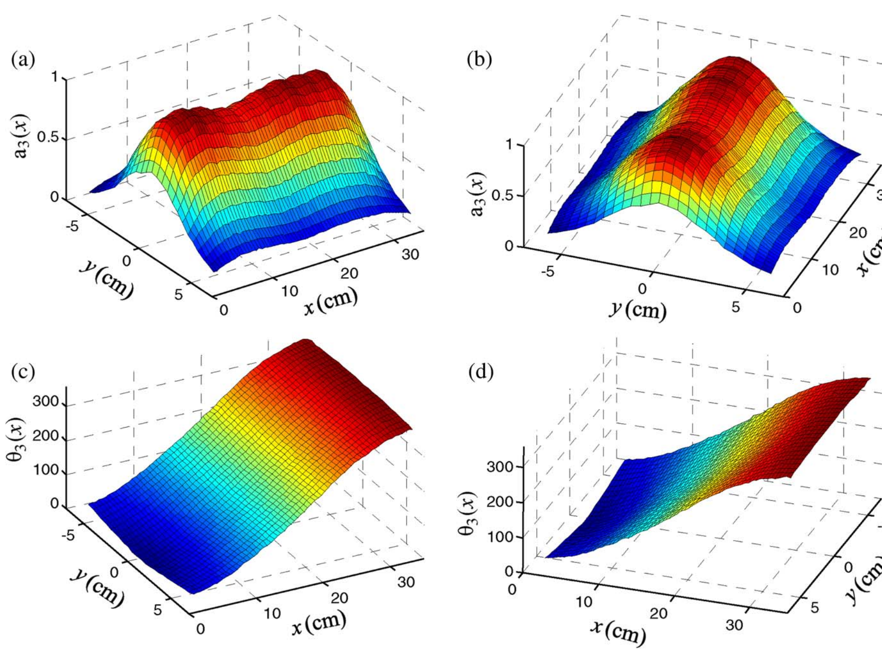

Fig. 8. (a) and (b) Light intensity and (c) and (d) phase are measured on the grid. Panels (a) and (b) are the same data but from a different viewing angle. Panels (c) and (d) are the same data but from a different viewing angle.

shows their corresponding phase values. For the same value of x, different y values should have different light intensities within the same phase. This means that even if the central visual field is offset in the y-axis, it still has the same EEG phase data. In other words, the acceptable range of the central visual field is not limited to $y = 0$.

5. Conclusion

This study proposes novel visual optics for VEP-based BCI using synthetic light to achieve a linear phase. Although the LCD screen has a phase from 0° to 360°, the central visual field phase can be reacted in the brain using cortical magnification [4], [5]. This means that EEG results can be used to identify user gaze location. The system must have a linear phase to use the simplest method of estimating the relationship between the EEG phase and the value of x. The BCI system can then predict the user gaze location. This system provides a visual method of controlling a computer cursor, allowing patients to operate a computer. The LCD screen measurement data confirm that the phase is approximately linear. The data prove that using a finite light source to achieve a linear phase is feasible. Fig. 7 shows that the difference between estimated x' and actual x error is small.

References

[1] E. T. Schmeisser, "Fractal analysis of steady-state-flicker visual evoked potentials: Feasibility," *J. Opt. Soc. Amer. A, Opt. Image Sci.*, vol. 10, no. 7, pp. 1637–1641, Jul. 1993.

[2] H. A. Baseler, E. E. Sutter, S. A. Klein, and T. Carney, "The topography of visual evoked response properties across the visual field," *Electroencephalogr. Clin. Neurophysiol.*, vol. 90, no. 1, pp. 65–81, Jan. 1994.

[3] B. Brown and M. Z. Yu, "Variation of topographic visually evoked potentials across the visual field," *Ophthal. Physl. Opt.*, vol. 17, no. 1, pp. 25–31, Jan. 1997.

[4] E. E. Sutter, "The brain response interface: Communication through visually-induced electrical brain responses," *J. Microcomput. Appl.*, vol. 15, no. 1, pp. 31–45, Jan. 1992.

[5] E. E. Sutter and D. Tran, "The field topography of ERG components in Man—I. The photopic luminance response," *Vis. Res.*, vol. 32, no. 3, pp. 433–446, Mar. 1992.

[6] G. Schalk, D. J. McFarland, T. Hinterberger, N. Birbaumer, and J. R. Wolpaw, "BCI2000: A general-purpose brain–computer interface (BCI) system," *IEEE Trans. Biomed. Eng.*, vol. 51, no. 6, pp. 1034–1043, Jun. 2004.

[7] J. V. Odom, M. Bach, C. Barber, M. Brigell, M. F. Marmor, A. P. Tormene, G. E. Holder, and Vaegan, "Visual evoked potentials standard (2004)," *Doc. Ophthalmol.*, vol. 108, no. 2, pp. 115–123, Mar. 2004.

[8] M. Cheng, X. Gao, S. Gao, and D. Xu, "Design and implementation of a brain–computer interface with high transfer rates," *IEEE Trans. Biomed. Eng.*, vol. 49, no. 10, pp. 1181–1186, Oct. 2002.

[9] E. C. Lalor, S. P. Kelly, C. Finucane, R. Burke, R. Smith, R. B. Reilly, and G. McDarby, "Steady-state VEP based brain–computer interface control in an immersive 3D gaming environment," *EURASIP J. Appl. Signal Process.*, vol. 2005, no. 1, pp. 3156–3164, Jan. 2005.

[10] P. Martinez, H. Bakardjian, and A. Cichocki, "Fully online multicommand brain–computer interface with visual neurofeedback using SSVEP paradigm," *Comput. Intell. Neurosci.*, vol. 2007, pp. 13–13, Jan. 2007.

[11] O. Friman, I. Volosyak, and A. Gräser, "Multiple channel detection of steady-state visual evoked potentials for brain–computer interfaces," *IEEE Trans. Biomed. Eng.*, vol. 54, no. 4, pp. 742–750, Apr. 2007.

[12] Y. Wang, R. Wang, X. Gao, B. Hong, and S. Gao, "A practical VEP-based brain–computer interface," *IEEE Trans. Neural Syst. Rehabil. Eng.*, vol. 14, no. 2, pp. 234–239, Jun. 2006.

[13] G. R. Muller-Putz, R. Scherer, C. Brauneis, and G. Pfurtscheller, "Steady-state visual evoked potential (SSVEP)-based communication: Impact of harmonic frequency components," *J. Neural Eng.*, vol. 2, no. 4, pp. 123–130, Dec. 2005.

[14] K. K. Shyu, P. L. Lee, Y. J. Liu, and J. J. Sie, "Dual-frequency steady-state visual evoked potential for brain computer interface," *Neurosci. Lett.*, vol. 483, no. 1, pp. 28–31, Oct. 2010.

[15] E. W. Sellers, D. J. Krusienski, D. J. McFarland, T. M. Vaughan, and J. R. Wolpaw, "A P300 event-related potential brain–computer interface (BCI): The effects of matrix size and inter stimulus interval on performance," *Biol. Psychol.*, vol. 73, no. 3, pp. 242–252, Oct. 2006.

[16] P. L. Lee, J. C. Hsieh, C. H. Wu, K. K. Shyu, S. S. Chen, T. C. Yeh, and Y. T. Wu, "The brain computer interface using flash visual evoked potential and independent component analysis," *Ann. Biomed. Eng.*, vol. 34, no. 10, pp. 1641–1654, Oct. 2006.

[17] F. Guo, B. Hong, X. Gao, and S. Gao, "A brain–computer interface using motion-onset visual evoked potential," *J. Neural Eng.*, vol. 5, no. 4, pp. 477–485, Dec. 2008.

[18] P. L. Lee, J. J. Sie, Y. J. Liu, C. H. Wu, M. H. Lee, C. H. Shu, P. H. Li, C. W. Sun, and K. K. Shyu, "An SSVEP-actuated brain computer interface using phase-tagged flickering sequences: A cursor system," *Ann. Biomed. Eng.*, vol. 38, no. 7, pp. 2383–2397, Jul. 2010.

[19] M. A. Lopez-Gordo, A. Prieto, F. Pelayo, and C. Morillas, "Use of phase in brain–computer interfaces based on steady-state visual evoked potentials," *Neural Process. Lett.*, vol. 32, no. 1, pp. 1–9, Aug. 2010.

[20] D. Zhu, G. Garcia-Molina, V. Mihajlovic, and R. M. Aarts, "Online BCI implementation of high-frequency phase modulated visual stimuli," in *Proc. 6th Int. Conf. Universal Access Human-Comput. Interact.*, 2011, pp. 645–654.

[21] K. K. Shyu, P. L. Lee, M. H. Lee, M. H. Lin, R. J. Lai, and Y. J. Chiu, "Development of a low-cost FPGA-based SSVEP BCI multimedia control system," *IEEE Trans. Biomed. Circuits Syst.*, vol. 4, no. 2, pp. 125–132, Apr. 2010.

[22] D. G. Stork and D. S. Falk, "Temporal impulse responses from flicker sensitivities," *J. Opt. Soc. Amer. A, Opt. Image Sci.*, vol. 4, no. 6, pp. 1130–1135, Jun. 1987.